

PAPER • OPEN ACCESS

## Nanofluids with Enhanced CHF Prepared from Self-Combustion Synthesized Al<sub>2</sub>O<sub>3</sub> Nanoparticles with PEG 1000 as Fuel

To cite this article: Dani Gustaman Syarif *et al* 2019 *IOP Conf. Ser.: Mater. Sci. Eng.* **515** 012046

View the [article online](#) for updates and enhancements.

# Nanofluids with Enhanced CHF Prepared from Self-Combustion Synthesized $\text{Al}_2\text{O}_3$ Nanoparticles with PEG 1000 as Fuel

**Dani Gustaman Syarif<sup>\*</sup>, Djoko Hadi Prajitno, Jupiter S. Pane**

Material Physics Group, Division of Technophysics, PSTNT BATAN, Jl. Tamansari No. 71, Bandung 40132. Telp. 022-2503997, Fax. 022-2504081

\*Corresponding author's email: danigus@batan.go.id

**Abstract.** To develop a new coolant for nuclear and non-nuclear applications, nanoparticles of  $\text{Al}_2\text{O}_3$  for nanofluids have been successfully synthesized using a self-combustion method from  $\text{Al}(\text{OH})_3$  precursor extracted from local bauxite. A sol was prepared by dissolving the  $\text{Al}(\text{OH})_3$  powder in water and adding an amount of PEG 1000 into the solution. The solution was stirred to form a sol and then was heated at 150 °C until forming a gel. The gel was then self-combusted at 450 °C and heated at 600 °C. The combusted and heated material was calcined at 1200 °C for 1 hour to get  $\text{Al}_2\text{O}_3$  nanoparticles. The preparation of nanofluids was done by dispersing the  $\text{Al}_2\text{O}_3$  nanoparticles into an amount of water as the base fluid. The  $\text{Al}_2\text{O}_3$  nanoparticles were crystallized in a theta phase with a crystallite size of 15.7 nm as confirmed by the XRD analyses. According to TEM data, it was known that the particle size of the nanoparticles was 35 nm. The nanofluid with the concentration of 0.025 vol % and pH of 10 possessed zeta potential of -42 mV indicating a stable suspension. This nanofluid had a CHF enhancement of 73% compared to water as the base fluid.

**Keywords:** Nanoparticle,  $\text{Al}_2\text{O}_3$ , bauxite, self-combustion, PEG 1000, nanofluid, CHF

## 1. Introduction

Various equipments that work with heat transfer systems such as nuclear reactors, automotive, air conditioners, have been familiar in everyday human life. The mentioned equipments require a cooling fluid which is then referred to as conventional fluids such as water, ethylene glycol, and oil. In heat transfer, the cooling fluids possess an important role. Currently, there is a tendency to increase the level of safety of the heat transfer system as well as its economic level. Various ways can be done to realize it but conventional ways such as increasing operating temperature and increasing surface area are considered uneconomical. The proper way is to replace the conventional fluids [1]. Some applications such as Reactor Vessel Cooling System (RVCS) and Emergency Core Cooling System (ECCS) in Nuclear Reactor [2], metal machining [3], and quenching [4,5] require fluids with large Critical Heat Flux (CHF). Other systems that require large CHF are air conditioning, refrigeration, thermal power generation, chemical engineering, aircraft and spacecraft thermal management, and high-power electronics component [1].



In 1995 for the first time, Choi introduced a new fluid known as nanofluid [6]. This fluid is developed based on nanotechnology. Nanofluid is a stable suspension formed by dispersion of nanoparticles with a size of 1-100 nm into the fluid. The important parts of the nanofluids are nanoparticles and base fluids. Various types of nanoparticles can be used for nanofluids including  $\text{Al}_2\text{O}_3$  [7-10],  $\text{ZrO}_2$  [11],  $\text{ZnO}$  [12],  $\text{SiO}_2$  [13],  $\text{Fe}_2\text{O}_3$  [14-15], and  $\text{Fe}_3\text{O}_4$  [16]. Meanwhile, the basic fluids can be water, ethylene glycol, oil, and glycerol. Among the various nanoparticles mentioned,  $\text{Al}_2\text{O}_3$  is very important and attractive because it has relatively large thermal conductivity and small thermal neutron absorption coefficient (for nuclear application) [17].

Currently, a lot of research related to  $\text{Al}_2\text{O}_3$  nanofluid has been done all over the world. The nanoparticles used were synthesized in various ways but were generally only intended to obtain very small particles (nanoparticles) and were not directly related to the nanofluid characteristics to be formed. A study has been done by the authors to prepare nanofluids of  $\text{Al}_2\text{O}_3$  by adjusting the characteristics of  $\text{Al}_2\text{O}_3$  nanoparticles with the sol-gel process [18] but the resulted nanofluid was still less stable. Good stability is required by a nanofluid to have large CHF. To solve this problem, in this research the preparation of  $\text{Al}_2\text{O}_3$  nanofluids from  $\text{Al}_2\text{O}_3$  nanoparticles of which surface characteristics were engineered by the synthesis of a self-combustion method was done by using Polyethylene glycol (PEG) 1000 as capping agent and fuel. The PEG 1000 could be a good source of minus charges for the  $\text{Al}_2\text{O}_3$  nanoparticles. The nanoparticles with the large surface charge will result in a stable nanofluid.

## 2. Methods

### 2.1. Material synthesis and characterization

The precursor of  $\text{Al}(\text{OH})_3$  was extracted from local bauxite using a method described in [6]. The powder of  $\text{Al}(\text{OH})_3$  was dissolved in the water inside a beaker glass. Then, a quantity of PEG 1000 was poured into the beaker glass containing  $\text{Al}(\text{OH})_3$  and stirred until it was completely soluble and forming a sol. The ratio of  $\text{Al}(\text{OH})_3$  and PEG 1000 was 1:0.25. The sol was heated at 150 °C to form a gel. Next, the gel was self-combusted at 450 °C and heated at 600 °C for 10 minutes. The visual appearance of the self-combustion process is shown in Figure 1. To obtain  $\text{Al}_2\text{O}_3$  nanoparticles, the self-combusted material was calcined at a temperature of 1200 °C for 1 hour. The visual appearance of the  $\text{Al}_2\text{O}_3$  nanoparticles as calcination product is depicted in Figure 2. The  $\text{Al}_2\text{O}_3$  nanoparticles were analyzed by X-ray Diffraction (XRD) to determine the crystal structure and to estimate the crystallite size. The XRD pattern was recorded with  $2\theta$  in the range of 10°-80° with  $\text{Cu-K}\alpha$ :  $\lambda = 1.5609 \text{ \AA}$ . The surface characteristic of the  $\text{Al}_2\text{O}_3$  nanoparticles was analyzed using a Fourier Transform Infrared spectrometer (FTIR), and the particle size was measured with the aid of a Transmission Electron Microscope (TEM).



**Figure 1.** The visual of the self-combustion process in this work

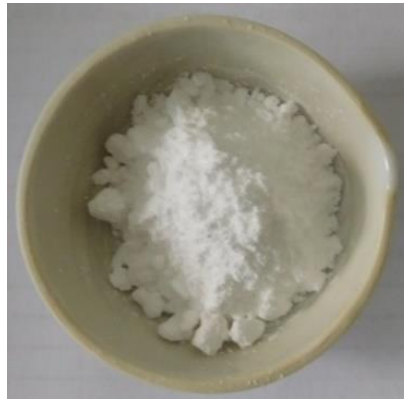


**Figure 2.** The visual appearance of Al<sub>2</sub>O<sub>3</sub> nanoparticles synthesized using the self-combustion method

### 2.2. Nanofluids preparation and characterization

An amount of 0.05 g of the Al<sub>2</sub>O<sub>3</sub> nanoparticles was dispersed into 100 ml distilled water as the base fluid. To obtain well-dispersed nanofluids, the mixtures were ultrasonicated for 2 hours. The pH of the nanofluids was measured using a Mettler Toledo pH meter. Subsequently, the other nanofluids with different nanoparticles weight namely 0.1 g and 0.4 g were prepared with the same step. The pH was adjusted using NH<sub>4</sub>OH to 10. Converting to vol % concentration was done by using Equation (1) [19].

$$\phi = \frac{m_p / \rho_p}{m_p / \rho_p + V_{BF}} \times 100\% \quad (1)$$

where,  $\phi$  is the Al<sub>2</sub>O<sub>3</sub> concentration in vol %,  $m_p$  is the mass of Al<sub>2</sub>O<sub>3</sub> nanoparticles,  $\rho_p$  is the density of Al<sub>2</sub>O<sub>3</sub>, and  $V_{BF}$  is the volume of the base fluid.

Zeta potential of the nanofluids was measured using a Zetasizer from Malvern. A digital camera was used to take pictures of the nanofluids. Critical Heat Flux (CHF) was measured using a method described in [7] utilizing Cu wire with a diameter of 0.1 mm. CHF enhancement was calculated using Equation (2) [7-8].

$$CHF_{enhancement} = \frac{CHF_{NF} - CHF_{BF}}{CHF_{BF}} \times 100\% \quad (2)$$

where  $CHF_{NF}$  is Critical Heat Flux of the nanofluids and  $CHF_{BF}$  is the base fluid (in this case water).

## 3. Results and Discussion

### 3.1. XRD analyses of Al<sub>2</sub>O<sub>3</sub> nanoparticles

A modified Bayer process was successfully used for extraction of Al(OH)<sub>3</sub> precursor from local bauxite. The XRD pattern of Al(OH)<sub>3</sub> is depicted in Figure 3. This Al(OH)<sub>3</sub> powder was then employed as a precursor in the synthesis of Al<sub>2</sub>O<sub>3</sub> nanoparticles using a self-combustion method. The formation of Al(OH)<sub>3</sub> indicated that the drying process of the precipitate resulted from precipitation step during the Bayer process was done at a low enough temperature. Usually, the precursor will be in the form of AlOOH (Boehmite) when dried at a higher drying temperature. However, both Al(OH)<sub>3</sub> (Gibbsite) and AlOOH (Boehmite) can be used as the precursor in a self-combustion process.

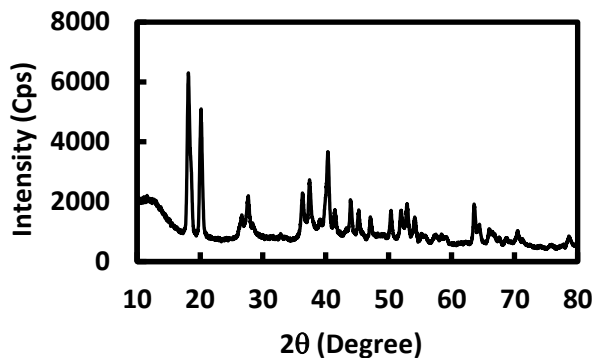


**Figure 3.** XRD pattern of  $\text{Al}(\text{OH})_3$  derived from local bauxite

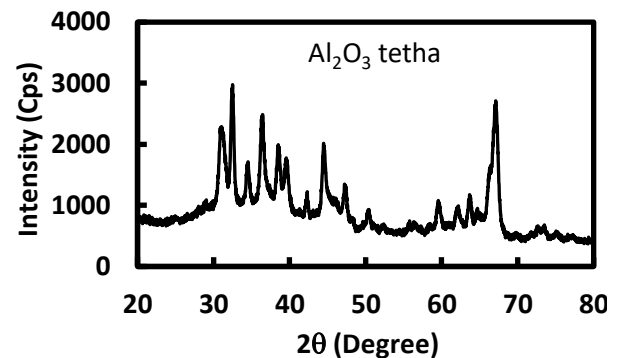


**Figure 4.** XRD pattern of  $\text{Al}_2\text{O}_3$  nanoparticles synthesized using the self-combustion with PEG 1000 as fuel calcined at 1200 °C for 1 hour. Crystallizes in the theta phase

Figure 4 shows the XRD pattern of the  $\text{Al}_2\text{O}_3$  nanoparticles synthesized using a self-combustion method utilizing PEG 1000 as fuel. The pattern was analyzed by comparing it to the XRD patterns from JCPDS. According to the analysis, it was known that the nanoparticles crystallized in the theta phase of  $\text{Al}_2\text{O}_3$  was in accordance with the JCPDS standard No. 23-1009. Based on the XRD pattern of Figure 4, a calculation was performed employing the Debye Scherrer method [7, 20] represented in Equation (3). The calculated average crystallite size was 15.7 nm.

$$D = \frac{0.9\lambda}{\beta \cdot \cos \theta} \quad (3)$$

where  $D$  represents the crystallite size of the nanoparticles,  $\beta$  represents the full width at half maximum (FWHM) in rad,  $\lambda$  of 0.15406 nm is the wavelength of X-rays, and  $\theta$  is the Bragg's angle (an angle of incidence).

With the same calcination temperature, the  $\text{Al}_2\text{O}_3$  nanoparticles synthesized in this work crystallized only in the theta phase while in our previous study [6] the  $\text{Al}_2\text{O}_3$  nanoparticles contained two phases, namely theta and alpha phases. This is due to the different method used. Therefore, the  $\text{Al}_2\text{O}_3$  nanoparticles in this work were purer compared to that in our previous study. However, compared to the crystallite size of the nanoparticle in our previous study, the crystallite size of the nanoparticle in this study was slightly larger but still comparable.

### 3.2. TEM analyses

The particle size was confirmed by a transmission electron microscopic (TEM) analysis. As shown in Figure 5, the average particle size of the as-prepared spherical shape  $\text{Al}_2\text{O}_3$  nanoparticles was 35 nm. The particles size was relatively small at a high calcination temperature (1200 °C) compared to that derived by Farahmandjou and Golabiyani with the calcination temperature of 600-1000 °C [15]. Our nanoparticles were more spherical than theirs. They utilized Aluminum nitrate as the precursor and glycine as fuel. The formation of the smaller spherical nanoparticles in this work indicated the role of PEG 1000 as a capping agent other than as a fuel. Hence, PEG 1000 is more effective with dual functions than glycine.

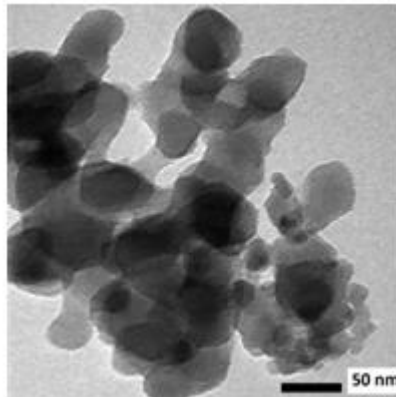


**Figure 5.** The TEM image of the  $\text{Al}_2\text{O}_3$  nanoparticles. The average size of the particles was 35 nm.

### 3.3. FTIR analyses of $\text{Al}_2\text{O}_3$ nanoparticles

Figure 6 depicts the FTIR spectra of  $\text{Al}_2\text{O}_3$  nanoparticles synthesized in this work. In the area of wavenumber of  $1500\text{--}4000\text{ cm}^{-1}$ , usually the presence of functional groups is identified. The wavenumber from  $600\text{--}1500\text{ cm}^{-1}$  is fingerprint region. The band of the bending vibration of O–H was found at around  $1620\text{ cm}^{-1}$ , and the band around  $3400\text{ cm}^{-1}$  corresponded to the stretching vibrations of surface adsorbed water and vibration bands of bonded hydroxyl groups [16]. The data of Figure 6 indicated the presence of the number of hydroxyl groups on the surface of  $\gamma$ -alumina nanoparticles. According to Figure 6, the characteristic vibration of  $\text{Al}_2\text{O}_3$  was confirmed by the presence of the stronger broadening bands from  $400$  to  $1000\text{ cm}^{-1}$  for  $\text{--Al--OH}$  and  $\text{--O--Al--O--Al--}$ . This characteristic was also found in a work of Khazaei et al. [21] and in our previous study [7].

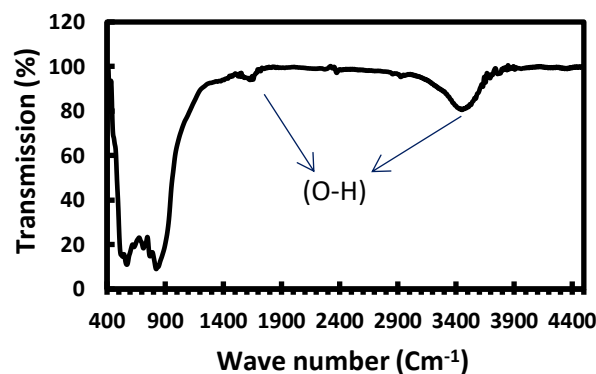


**Figure 6.** The FTIR spectra of as-synthesized nanoparticles with a calcination temperature of  $1200\text{ }^\circ\text{C}$

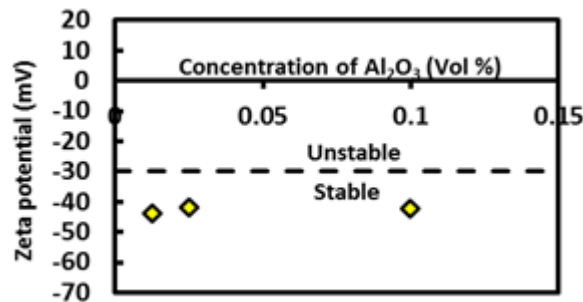
### 3.4. Characterization of $\text{Al}_2\text{O}_3$ nanofluids

Figure 7 displays a visual appearance of the nanofluids as the function of  $\text{Al}_2\text{O}_3$  concentrations. The first bottle contained nanofluid with the  $\text{Al}_2\text{O}_3$  concentration of  $0.0125\%$  vol while the second and third bottle contained nanofluid with the  $\text{Al}_2\text{O}_3$  concentration of  $0.025\%$  vol and  $0.1\%$  vol, respectively. The degree of white color changed with the concentration of the nanoparticles. The higher the concentration of the nanoparticles, the more white the color. Figure 8 depicts the nanofluids zeta potential at different concentrations of  $\text{Al}_2\text{O}_3$  nanoparticles. A suspension can be stable since possessing zeta potential larger than  $30\text{ mV}$  or smaller than  $-30\text{ mV}$ . As shown in Figure 8, the zeta potential of the nanofluids in this work met that criterion indicating that the nanofluids were stable. The minus zeta potential suggested that the nanofluids were basic. The charges originated from  $\text{OH}^-$  were distributed on the surface of the nanoparticles in the nanofluids. The zeta potential increased with the minus charges on the surface of the particles. The larger zeta potential reflected the repulsion force between nanoparticles in nanofluid

would be larger as well. As the consequence, the larger the zeta potential, the nanofluids would be more stable. The population of OH<sup>-</sup> on the surface of the nanoparticles is influenced by the synthesis process of the Al<sub>2</sub>O<sub>3</sub> nanoparticles [7]. In this work, the OH<sup>-</sup> formation was caused by the PEG 1000 used as the capping agent and fuel during synthesis of the Al<sub>2</sub>O<sub>3</sub> nanoparticles.



**Figure 7.** The visual appearance of the nanofluids with the different concentrations of the Al<sub>2</sub>O<sub>3</sub> nanoparticles after preparation. From left, the first to third bottles are nanofluid with the Al<sub>2</sub>O<sub>3</sub> concentration of 0.0125 % vol, 0.025 % vol, and 0.1 % vol, respectively.



**Figure 8.** Zeta potential of Al<sub>2</sub>O<sub>3</sub> nanofluids at different Al<sub>2</sub>O<sub>3</sub> concentrations.

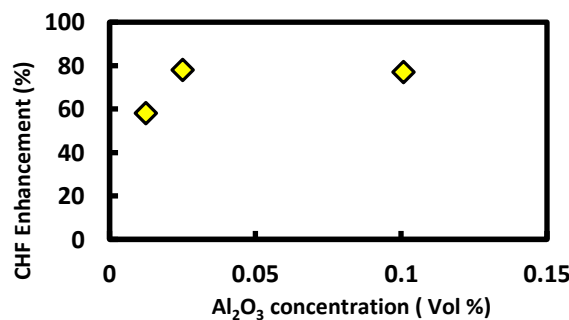


**Figure 9.** CHF enhancement of Al<sub>2</sub>O<sub>3</sub> nanofluids at different Al<sub>2</sub>O<sub>3</sub> concentrations

Figure 7 displays the CHF enhancement of the nanofluids as the function of Al<sub>2</sub>O<sub>3</sub> nanoparticles concentration. The Al<sub>2</sub>O<sub>3</sub> nanoparticles were coated on the surface of Cu wire. The nanoparticles coating increased the wettability of the Cu surface causing the heat transfer from the wire to the nanofluid larger. The increase in wettability delayed the departure of water from the wire surface. This condition makes the CHF increased. The detailed CHF enhancement of Al<sub>2</sub>O<sub>3</sub> nanofluids at different

Al<sub>2</sub>O<sub>3</sub> concentrations can be seen in Figure 9. At a low concentration of Al<sub>2</sub>O<sub>3</sub>, the increase in the concentration was followed by the increase in the CHF enhancement, however, at further concentration, the CHF enhancement did not change. This means that there was an optimal concentration. At a higher concentration, the large population of the nanoparticles tended to decrease the wettability. Compared to our previous study [2], the CHF enhancement of the nanofluids in this work was slightly smaller. This was due to the smaller zeta potential and larger particle size. Compared to our previous study, the particles size of the nanoparticles in this work was larger. However, compared to some reported studies [18], the CHF enhancement of the nanofluids in this study was comparable and large enough.

A literature shows the benefit of the application of nanofluids in metal machining [3] covering drilling, turning, milling, and drilling. According to Shokoohi and Shekarian nanofluids can reduce cutting force, machining temperature, tool wear, and surface roughness in metal machining process [3]. The nanofluids in this work are potential to be applied in the metal machining process. Bang and Kim reported [2] that their nanofluid with the cooling rate (230 °C/s) that was faster than pure water (218 °C/s) may be applied for RVCS and ECCS application. By the enhanced CHF, the nanofluids prepared in this work are also possible to be applied in RVCS and ECCS.

#### 4. Conclusion

Nanoparticles of theta Al<sub>2</sub>O<sub>3</sub> with the particle size of 35 nm have been well synthesized using a self-combustion method utilizing PEG 1000 as a fuel. PEG 1000 showed a good performance as a capping agent and fuel in the self-combustion process. Nanofluids were prepared by utilizing these Al<sub>2</sub>O<sub>3</sub> nanoparticles with pH 10 that possessed zeta potential of -42 to -44 mV indicating stable suspensions. The nanofluids had CHF enhancement of 58-78%. With this characteristic, the nanofluids are potential for cooling fluids of metal machining, quenching, RVCS, and ECCS.

#### References

- [1] Fang X D, Chen, Y F, Zhang H L, Chen W W, Dong A Q, Wang R 2016, *Renewable and Sustainable Energy Reviews* 62, 924–940
- [2] Bang I C, Kim J H 2011, IAEA-CN-164-5S10
- [3] Shokoohi Y, Shekarian E 2016 *J Nanosci Technol* 2(1), 59–63
- [4] Patra N, Gupta V, Singh R, Singh R S, Ghosh P, Nayak A 2017 *Resource-Efficient Technol* (2017), doi: 10.1016/j.reffit.2017.02.006
- [5] Ramesh G and Prabhu N K 2011 *Nanoscale Res Lett* 2011, 6:334
- [6] Choi, SUS, Eastman J A 1995 ASME International Mechanical Engineering Congress and Exposition, November 12–17, 1995, San Francisco, CA
- [7] Syarif D G, Prajitno D H, Pane J S 2018 *J Aus Ceram Soc* 54 (1), 47-53
- [8] Syarif D G. 2016 *J Phys: Conference Series* 776, 012042
- [9] Esfe M H, Karimipour A, Yan W M, Akbari M, Safei M R, Dahari M 2015 *Int. J. Heat Mass Tran* 88, 728–734
- [10] Sarafraz M M, Hormozi F 2014 *Int Commun Heat Mass Tran* 58, 96–104.
- [11] Chopkar M, Das A K, Manna I., Das P K 2008 *Heat Mass Transfer* 44:999–1004
- [12] Saleh R, Putra N, Prakoso S P, Septiadi W N 2013 *Int J Therm Sci* 63, 125–132
- [13] Akbai M, Afrand M, Arshi A, Karimipour A 2017 *J Molec Liq* 233, 352-357
- [14] Guo S Z, Li Y, Jiang J S, Xie H Q 2010 *Nanoscale Res Lett* 5, 1222–1227
- [15] Colla L, Fedele L, Scattolini M, Bobbo S 2012 *Adv Mech Eng* 2012, 674947 (2012)
- [16] Syarif D G, Prajitno D H 2016 *J Aust Ceram Soc* Vol. 52(2), 76–81
- [17] Syarif D G 2016 BATAN Press (In Indonesian)
- [18] Syarif D G, Prajitno D H, Umar E *Materials Science Forum* 929, pp 1-9
- [19] Al-Waelia A H A, Chaichan M T, Kazem H A, Sopiana K, Safaiea J 2018 *Case Studies in Thermal Engineering* 12, 405–413
- [20] Ravikumar B S, Nagabhusana H, Sharma S C, Vidya Y S, Anantharaja K S 2015 *Spectrochimica Acta Part A: Molecular and Biomolecular Spectroscopy* 136,1027-1037.

- [21] Khazaei A, Nazari S, Karimi G, Ghaderi F, Moradian K M, Bagherpor Z, Nazari S 2016 Int J Nanosci Nanotechnol. 12(4), 207– 214

### **Acknowledgments**

The authors are very grateful to the government of the Republic of Indonesia for funding this research through DIPA BATAN program year 2017-2018.